Defining Characteristics of Nodal Disease on PET/CT Scans in Patients With HIV-Positive and -Negative Locally Advanced Cervical Cancer in South Africa

Carrie Anne Minnaar[1], Ans Baeyens[1,2], Olusegun Akinwale Ayeni[3], Jeffrey Allan Kotzen[4], and Mboyo-Di-Tamba Vangu[5]

[1]Division of Radiobiology, Department of Radiation Sciences, University of the Witwatersrand, Johannesburg, South Africa; [2]Division of Radiobiology, Department of Human Structure and Repair, Ghent University, Ghent, Belgium; [3]Department of Nuclear Medicine, Charlotte Maxeke Johannesburg Academic Hospital, Johannesburg, South Africa; [4]Department of Radiation Oncology, Wits Donald Gordon Medical Centre, Johannesburg, South Africa; and [5]Department of Nuclear Medicine, Department of Radiation Sciences, University of the Witwatersrand, Johannesburg, South Africa

Corresponding Author:
Ans Baeyens, PhD
Division of Radiobiology, Department of Human Structure and Repair, Gent University, Entrance 46, building 6B3, C. Heymanslaan 10, 9000 Gent, Belgium,
E-mail: Ans.Baeyens@UGent.be; and Ans.Baeyens@wits.ac.za

Key Words: ^{18}F-FDG PET/CT, HIV, locally advanced cervical cancer, lymph nodes, disease pattern

Abbreviations: ^{18}Flourine-labeled 18-fluoro-2-deoxyglucose (^{18}F-FDG), acquired immunodeficiency syndrome (AIDS), antiretroviral therapy (ART), computed tomography (CT), International Federation of Gynecology and Obstetrics (FIGO), human immunodeficiency virus (HIV), locally advanced cervical cancer (LACC), position emission tomography (PET), standardized uptake value (SUV), maximum SUV (SUVmax)

ABSTRACT

Literature reports increased FDG nodal uptake in HIV-positive patients. Our aim is to identify differences in presentation and characteristics of FDG-avid lymph nodes between HIV-positive and HIV-negative locally advanced cervical cancer (LACC) patients in our clinical setting. We evaluated 250 pre-treatment ^{18}F-FDG PET/CT imaging studies from women screened for a phase III randomised controlled trial investigating modulated electro-hyperthermia as a radiosensitiser (Ethics approval: M120477). The number of nodes; size; maximum standardised uptake value (SUVmax); symmetry; and relationship between nodal size and SUVmax uptake, were assessed by region and by HIV status. In total, 1314 nodes with a SUVmax $\geq$ 2.5 were visualised. Of 128(51%) HIV-positive participants, 82% were on antiretroviral therapy (ART) and 10 had a CD4 count <200 cells/μL. Overall pattern of presentation and nodal characteristics were similar between HIV-positive and -negative groups and the uniformity in presentation of the nodes draining the cervix strongly suggests these nodes may be attributed to malignancy rather than HIV infection. Novel findings: HIV infection is associated with: >four nodes visualised in the neck, symmetrical inguinal lymph nodes, increased rates of supraclavicular node visualisation; FDG-avid axillary nodes were more common, but not exclusive, in HIV-positive participants. ^{18}F-FDG PET/CT is a reliable staging method for LACC in HIV-positive patients who are not in acute stages of HIV infection, have a CD4 count >200 cells/μL, and/or are on ART and there is a potential risk of underestimating metastatic spread by attributing increased nodal metabolic activity to HIV infection in these patients.

INTRODUCTION

Position emission tomography (PET) is an imaging modality that uses a tomographic technique to measure the 3-dimensional distribution of positron-emitting labeled radiotracers. ^{18}Flourine-labeled glucose (18-fluoro-2-deoxyglucose; ^{18}F-FDG) is the most commonly used tracer for PET studies. Most cancers characteristically have increased utilization of glucose, upregulation of glucose transporters, and consequently an increased uptake of glucose analogue FDG on PET studies. This allows for the noninvasive quantification of tumor metabolic activity, measured by the standardized uptake value (SUV) of FDG by the tumor compared with the FDG uptake value of background tissues. The addition of computed tomography (CT) allows the morphological evaluation of the tumor to improve the accuracy of the size and localization, combined with the metabolic measurement on the PET images (1).

One advantage of ^{18}F-FDG PET/CT is its ability to detect metabolic changes before anatomical changes occur, making it more sensitive to the nodal disease status of patients (2, 3). In

The corresponding author had full access to all the data and was responsible for the final submission.

ISSN 2379-1381 https://doi.org/10.18383/j.tom.2019.00017

the developed world, several studies have assessed the role of ^{18}F-FDG PET/CT in the staging and management of patients with locally advanced cervical cancer (LACC), and results from ^{18}F-FDG PET/CT scans can provide important prognostic information for these patients with cervical cancer (4). The staging of cervical cancer is based on the FIGO (International Federation of Gynecology and Obstetrics) classification, which is a clinical staging system involving a thorough clinical examination and anatomical imaging. In a resource-constrained setting, a chest x-ray, abdominal ultrasonography, and cystoscopy are routinely performed on patients with cervical cancer with further investigations considered on a case-by-case basis, and depending on resources and availability (5).

Morkel et al. reported that the addition of ^{18}F-FDG PET/CT to the initial screening protocols for patients with FIGO stage IIIB cervical cancer revealed relevant disease information that was missed by clinical staging and other imaging techniques. The information gathered from the ^{18}F-FDG PET/CT resulted in a change in treatment protocols in a significant number of patients with cervical cancer (5). In a study by Kidd et al., 53% of the 234 patients with cervical cancer (FIGO stage IB1–IVA), had FDG-avid lymph nodes on ^{18}F-FDG PET/CT scans, with nodes visualized as high as the supraclavicular region. Lymph node status as visualized on the ^{18}F-FDG PET/CT scans had a significant effect on patient outcomes, and the presence and number of lymph node metastases are known prognostic factors (6, 7). The sensitivity of the PET/CT studies depends on the stage of disease, with limited benefit of the use of ^{18}F-FDG PET/CT scans seen in early stages of cervical cancer (8-10). The typical metastatic pattern for cervical cancer is from the nodes directly draining the cervix (parametrium and paracervix), to the external iliac, internal iliac, obturator, and mesorectum groups (sometimes referred to as level one), to the common iliac and presacral groups (or level two groups), to para-aortic nodes (level three) (11-13).

A well-known challenge regarding the interpretation of ^{18}F-FDG PET/CT scans is the risk of false-positive results in patients with acute infections or inflammatory conditions (14). Activated inflammatory cells, such as macrophages, lymphocytes, neutrophil granulocytes, and fibroblasts, have been shown to avidly take up FDG, resulting in an FDG uptake that is higher than the background uptake (15). The gradual decrease in CD4 cells of human immunodeficiency virus (HIV)-1-infected individuals is associated with a decline in the function of patient's immune system. The homing theory suggests that the homing of HIV-infected CD4 cells from the blood to the lymph nodes where they undergo apoptosis is a possible cause for the decrease in CD4 counts (16, 17). This correlates with generalized lymphadenopathy typically seen in HIV-infected patients.

Studies have shown the importance of taking the HIV status of the patient into account when interpreting the results of ^{18}F-FDG PET/CT images of patients with cancer. Morkel et al. found a significant inverse relationship between the CD4 count of HIV-positive patients and the mean SUV of their lymph nodes (5), and another study found that HIV-positive patients with high viral load levels may have benign hypermetabolic foci visualized on ^{18}F-FDG PET/CT images (18). This may result in false-positive interpretations of malignancy. Increased FDG uptake of the lymphoid tissue is seen in the head and neck region during acute HIV infection, in the peripheral nodes (including the axillary and inguinal nodes) during chronic infection, and in the abdominal lymph nodes during late stages of HIV infection (18-20). A detailed study by Brust et al. showed that healthy HIV-infected individuals with suppressed viral loads, and their HIV-negative counterparts, had little to no FDG uptake in lymph nodes; however, HIV-positive patients with high viral loads and advanced HIV infection had increased FDG uptake in the peripheral lymph nodes (21).

To the best of our knowledge, there are no larger studies investigating the nodal characteristics and distribution patterns of HIV-positive, compared to HIV-negative, patients with LACC in a resource-constrained setting. In this paper, we report on the results of ^{18}F-FDG PET/CT images from participants enrolled in an ongoing phase III randomized controlled trial on the effects of the addition of modulated electro-hyperthermia to chemoradiation protocols in South Africa. We aim to identify differences in the characteristics of positive lymph nodes between HIV-positive and HIV-negative LACC participants. This may assist in more accurate reporting and staging of cervical cancer on ^{18}F-FDG PET/CT studies in geographic areas with a high incidence of HIV infection.

MATERIALS AND METHODS

The data for this analysis are part of a phase III randomized controlled trial investigating the addition of modulated electrohyperthermia to chemoradiotherapy for the treatment of patients with LACC. The trial is being conducted in our local academic hospital by the Department of Radiation Sciences of the University of the Witwatersrand, Johannesburg, South Africa. All procedures performed in studies involving human participants were in accordance with the ethical standards of the institutional/national research committee (Human Research Ethics Committee approval: M120477) and the 1964 Helsinki declaration and its later amendments or comparable ethical standards. The trial was registered on the South African National Clinical Trials Register before recruitment started (ID: 3012) and at ClincialTrials.gov ID: NCT03332069. Informed consent was obtained from all individual participants included in the study.

Eligibility

As part of the screening evaluation for the trial protocol, potential participants had additional hematological investigations including HIV tests and CD4 count, and they underwent ^{18}F-FDG PET/CT imaging studies before randomization, but only after signing the informed consent.

Patients were considered eligible for screening for the trial and were therefore found eligible for this analysis if they were>18 years old, with histologically confirmed squamous cell carcinoma of the cervix, FIGO stage IIB (with distal involvement of the parametrium) to IIIB (staged clinically), creatinine clearance of >60 mL/min, reported knowing their HIV-status, did not have any AIDS-defining illnesses except for cervical cancer, were deemed fit for treatment with radical intent, and had a life expectancy of >12 months.

Once the screening process was complete, exclusion criteria for randomization for the trial based on the screening results

included a CD4 count of <200 cells/μL if HIV-positive, visceral metastatic disease, bilateral hydronephrosis, or fistulas visualized on ^{18}F-FDG PET/CT scans.

In total, 270 participants were screened, 250 of whom underwent pretreatment ^{18}F-FDG PET/CT imaging studies, and 210 were deemed eligible for trial and were randomized for treatment. For the purpose of this report, we evaluated all 250 of the ^{18}F-FDG PET/CT imaging studies conducted as part of the screening process.

Patient Preparation and Imaging Protocol

Participants were prepared for the ^{18}F-FDG PET/CT scans according to department standard protocols. Plasma glucose was checked before the scan, and hydration was administered to participants whose plasma glucose levels were ≥11 mmol/L or more to lower glucose levels and minimize the interference by high glucose (1). The PET/CT study was rescheduled if the plasma glucose could not be adequately lowered. Our protocol aimed for an uptake period of ±1 h between injection and scanning (1) depending on the logistics. Participants were injected with a mean of 378.51 MBq (minimum, 135.79 MBq; maximum, 462.5 MBq) of FDG. The participants' mean plasma glucose level was 5.7 mmol/L (minimum, 3.7 mmol/L; maximum, 12.2 mmol/L), and there was a mean interval of 66.5 min (minimum, 50; maximum, 125) between injection time and acquisition of body image.

The scanning protocol begins with a scout image, followed by a low-dose CT image (with intravenous contrast when not contraindicated) of the whole body. This was followed by "whole-body" PET imaging in 7 bed positions, 3 min per bed, starting from mid-thigh to the base of the skull. A diagnostic CT of the chest was then performed. The ^{18}F-FDG PET/CT scans were obtained using a Siemens Biograph^{TM} 40 PET/CT (Siemens Healthcare GmbH; Erlangen, Germany).

Nodal Analysis

The nodal characteristics assessed included number of nodes and their largest diameter on CT scans, uptake assessed by measured maximum SUV (SUVmax), symmetry, and relationship between nodal size and SUVmax uptake. SUVmax ≥ 2.5 was used as a cutoff for active nodes. Patterns were compared between different anatomical regions that included the pelvis, abdomen, thorax, and head and neck. First, the characteristics of all of the nodes were analyzed depending on whether the node appeared in the HIV-negative or -positive participants (nodal analysis). Then the participants in each group (HIV-positive and HIV-negative) were assessed, and the characteristics of their nodes were compared (participant analysis). A subgroup analysis of specific node groups responsible for the drainage of the cervix and nodes known to be positive in HIV infection was conducted.

Statistics

Frequencies and percentages were calculated, and we used chi-square frequency tables, unpaired *t* test, linear regression and logistic regression models to measure associations, differences, and odds ratios. STATA 13.0 Statistics software program (Stata Corporation, College Station, TX) was used to analyze the data.

Funding

This study was funded by the National Research Foundation of South Africa (TP12082710852). ^{18}F-FDG was supplied at a discounted rate by Radioisotopes SOC Ltd. NTP Radioisotopes SOC Ltd is a state owned company and a subsidiary of the South African Nuclear Energy Corporation. The company manufactures and supplies radioisotopes. Funding sources had no role in study design, implementation, data collection, and data analysis or development/review of the manuscript.

RESULTS

Participant characteristics are listed in Table 1. Majority of the participants were African (92%); 128 (51%) were HIV-positive, 119 (82%) of whom were on antiretroviral therapy (ART) at the time of the scan. The median CD4 count was 506.5 cells/μL (range, 95–1524 cells/μL), and 10 participants had a CD4 count <200 cells/μL.

Overall Nodal Analysis

In total, 2299 nodes were visualized, 1314 of which had SUVmax ≥ 2.5 and were included in the analysis (HIV-positive, 713 [54%]; HIV-negative, 601[46%]). A summary of the number of nodes per region, and of the HIV status of the participant in which the node was visualized, can be seen in Table 2.

SUVmax Analysis by Region. Overall, the mean SUVmax was significantly higher in the pelvis and the abdomen compared with the head and neck region ($P < .001$) and thorax ($P < .001$). However the difference in SUVmax between the abdominal and pelvic nodes was not significant ($P = .397$). The mean SUVmax was the highest in the pelvis, and this was significantly higher than that in any other region ($P < .001$).

SUV and HIV Status. When considering all nodes, in a multivariate logistic regression analysis, a higher SUVmax was a predictor of the HIV status of the participants in which the node was visualized (OR, 0.97; $P = .022$; 95% CI, 0.945–0.996). However when considering the nodes by region, the abdomen was the only region in which the SUVmax of the nodes was predictive of the HIV status of the participants (OR, 0.92; $P = .006$; 95% CI, 0.86–0.98). When considering the SUVmax of all of the visualized lymph nodes, grouped into bins of 10 starting from 3, HIV-negative participants were more likely to have SUVmax of between 3 and 23 and SUVmax > 23 is associated with an HIV-positive status (chi-square: $P = .028$). The association was however not significant in a chi-square analysis of each region. In HIV-positive participants, the relationship between SUVmax and CD4 count was not significant ($P = .131$; 95% CI, −0.003 to 0.0003).

Size Analysis by Region. The largest nodes were seen in the pelvis, and the difference in sizes between the pelvic and abdominal nodes was significant ($P < .0001$). The lymph nodes in the abdomen were significantly larger than the nodes of the thorax ($P = .0047$) and those in the head and neck ($P < .0001$).

Size and HIV Status. When considering the size of the nodes (in centimeters), grouped into 0.5-cm bins, the only significant finding was that the nodes from the abdomen of HIV-positive participants are more likely to be <1.49 cm (106 out of 146 vs 80 out of 142), and the nodes from HIV-negative participants are more likely to be 1.49 cm–2.49 cm (51 out of 145 vs 28 out of 142; chi-square: $P = .027$). In a logistic regression analysis, lymph node size was not predictive of the HIV status; however, the increased size was

Table 1. Participant Characteristics[a]

		Overall		HIV-Positive		HIV-Negative		P Value
		n	[%]	n	[%]	n	[%]	
		250		128	[51%]	122	[49%]	
ECOG Performance Status	0	10	[4%]	5	[3.9%]	5	[4%]	χ^2: $P = 0.382$
	1	238	[95%]	121	[94.5%]	117	[96%]	
	2	2	[1%]	2	[1.6%]	0	[0%]	
Race	African	*229*	*[92%]*	*123*	*[96%]*	*106*	*[87%]*	χ^2: $P = 0.004$
	Caucasian	*10*	*[4%]*	*0*	*[0%]*	*10*	*[8%]*	
	Other	*11*	*[4%]*	*5*	*[4%]*	*6*	*[5%]*	
Age (years)	Median	*47.7*		*43.2*		*52.5*		t-test: $p<0.0001$
	Range	25.9–72.7		26.6–62.4		25.9–72.7		
BMI	Median	*26*		*24*		*28*		t-test: $P = 0.0032$
	Range	15–49		5–47		15–49		
CD4 count (cells/μL)	Median	506.5		506.5				
	Range	95–1524		95–1524				

Abbreviations: BMI: Body Mass Index; HIV: Human Immunodeficiency Virus; ECOG: Eastern Cooperative Oncology Group.
[a] Characteristics of the participants in the study: ECOG performance was similar in both groups; there were significantly more African HIV-positive participants and more Caucasian HIV-negative participants; the mean age and BMI was significantly higher in the HIV-negative participants.

significantly associated with reduced CD4 counts in HIV-positive participants (coefficient, −21.34; $P = .033$; 95% CI, 40.94 to 1.75): Supplemental Image 3 is of the participant (42) who was HIV-positive and had the highest SUV measured in a lymph node (54.2).

Relationship Between SUV and Size. The mean size of the visualized nodes was 1.55 cm (standard deviation [SD], 0.93; minimum, 0.5 cm; maximum, 14.2 cm chain of nodes) and the mean SUVmax was 6.43 (SD, 4.87; minimum, 2.5; maximum, 54.21). There is a moderately strong ($r = 0.5$) and significant ($P < .001$) positive relationship between the overall SUVmax and node diameter. This relationship was significant for each region, regardless of the HIV status, when analyzed independent of the participants and when analyzed per participant (Figure 1).

Analysis of Lymph Nodes Within Participants (Participant Analysis)

In paired *t*-test analyses, the maximum size of the nodes, the maximum SUVmax of the nodes, and the number of nodes overall and by region were assessed in each participant. There were no significant differences in the numbers of nodes in HIV-positive participants compared with HIV-negative participants ($P > .05$). These results are summarized in Table 3 and represented graphically in online supplemental Images 1, 2, and 4. To determine if there is any association between HIV status and a specific size or SUVmax, nodes were organized into bins and frequency tables were

Table 2. Number of Nodes per Region and the HIV Status of the Participant in Which the Nodes Were Visualized[a]

	Total	HIV-Positive		HIV-Negative	
Head and Neck	225	139	[62%]	86	[38%]
Thorax	210	115	[55%]	96	[45%]
Abdomen	293	149	[51%]	144	[49%]
Pelvis	586	310	[53%]	276	[47%]
Total number of nodes	1314	713	[54%]	601	[46%]

[a] Overall there were more nodes visualized in HIV-positive participants, with the largest difference in the number of nodes between HIV-positive and -negative participants seen in the head and neck region.

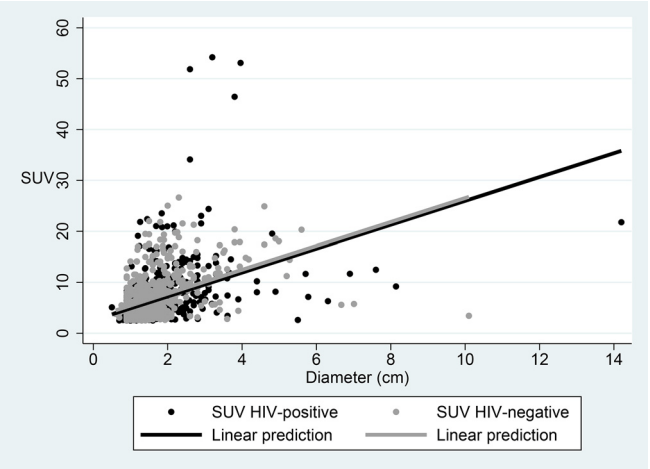

Figure 1. Linear relationship between the SUVmax and size of the lymph nodes in HIV-positive and -negative participants. A significant ($P < .001$) positive association is seen between the SUVmax of the lymph node and the diameter of the lymph node, and this relationship is independent of HIV status.

Table 3. Comparison of Means Summary of Nodes Per Participant[a]

	HIV-Positive (n = 128)		HIV-Negative (n = 122)		
	Mean	**SD**	**Mean**	**SD**	***t*-test**
Head and Neck	**n = 51**	**[40%]**	**n = 43**	**[35%]**	***P* = 0.453**
No Nodes Per participant	1.09	1.88	0.71	1.31	*P* = 0.0652
SUVmax	4.48	2.05	4.68	2.86	*P* = 0.6869
Diameter	1.17	0.29	1.21	0.36	*P* = 0.5964
Highest SUVmax	5.63	4.07	5.69	4.60	*P* = 0.9442
Maximum Diameter	1.41	0.55	1.34	0.54	*P* = 0.5256
Thorax	**n = 54**	**[42%]**	**n = 44**	**[36%]**	***P* = 0.322**
No Nodes Per participant	0.90	1.35	0.78	1.31	*P* = 0.4774
SUVmax	5.14	3.09	4.93	3.25	*P* = 0.7473
Diameter	1.42	0.66	1.29	0.47	*P* = 0.2707
Highest SUVmax	5.86	3.65	5.70	3.98	*P* = 0.8300
Maximum Diameter	1.74	1.85	1.49	0.69	*P* = 0.4017
Abdomen	**n = 68**	**[53%]**	**n = 62**	**[51%]**	***P* = 0.715**
No Nodes Per participant	1.16	1.44	1.18	1.55	*P* = 0.9315
SUVmax	6.65	4.50	7.67	4.38	*P* = 0.1940
Diameter	1.45	0.69	1.55	0.85	*P* = 0.4334
Highest SUVmax	7.85	5.26	9.11	5.35	*P* = 1.1779
Maximum Diameter	1.77	1.21	1.89	1.23	*P* = 0.5763
Pelvis	**n = 99**	**[77%]**	**n = 98**	**[80%]**	***P* = 0.564**
No Nodes Per participant	2.42	2.06	2.26	1.89	*P* = 0.5248
SUVmax	6.76	4.09	6.79	3.60	*P* = 0.9471
Diameter	1.70	0.73	1.69	0.76	*P* = 0.9218
Highest SUVmax	9.22	6.90	8.90	5.50	*P* = 0.7212
Maximum Diameter	2.27	1.30	2.20	1.34	*P* = 0.7073
Total	**n = 114**	**[89%]**	**n = 111**	**[91%]**	**χ^2: *P* = 0.613**
No Nodes Per participant	5.57	4.74	4.93	4.54	*P* = 0.2739
SUVmax	3.57	2.44	3.51	2.54	*P* = 0.8676
Diameter	0.88	0.49	0.83	0.48	*P* = 0.4424
Highest SUVmax	9.67	7.05	9.44	5.89	*P* = 0.7911
Maximum Diameter	2.48	1.78	2.32	1.41	*P* = 0.4488

Abbreviations: SD, standard deviation; SUV, standardized uptake value.
[a] There were no significant differences seen between the number of nodes per participant, maximum SUV uptake, and maximum diameter of the visualized lymph nodes between HIV-positive and HIV-negative participants.

generated. No significant association was seen when looking at participants' maximum or mean size or SUVmax. The only significant association between HIV status and number of lymph nodes in participant was seen in the head and neck region, where >4 nodes are more strongly associated with HIV infection (chi-square: $P = .004$).

Subgroup Analysis

A subgroup analysis of specific lymph node groups known to be positive on ^{18}F-FDG PET/CT in HIV-positive patients to determine whether, in our sample, there is a risk of understaging of the cervical cancer by attributing positive nodes to HIV-infection rather than malignancy was conducted.

Head and Neck Nodes (Known to Be Positive in Early HIV Infection). Of specific interest in the head and neck region was the significantly higher number of supraclavicular nodes visualized in HIV-positive participants (mean, 0.15; SD, 0.454; 95% CI, 0.069–0.228) compared with the number of those in HIV-negative participants (mean, 0.05; SD, 0.217; 95% CI, 0.01–0.09) ($P = .0296$). Posterior cervical nodes were also visualized significantly more ($P = .0037$) in HIV-positive participants (mean, 0.21; SD, 0.053; 95% CI, 0.107–0.315) than in HIV-negative participants (mean, 0.04; SD, 0.022; 95% CI, 0.002–0.084). Online supplemental Images 5a and 5b are of the HIV-positive (5a) and HIV-negative (5b) participants with the highest number of lymph nodes visualized in the head and neck region.

Axillary Nodes (Known to Be Positive in Chronic HIV Infection). Seven out of 122 (6%) HIV-negative and 29 out of 128 (23%) HIV-positive participants presented with axillary nodes visualized on ^{18}F-FDG PET/CT scans. In a logistic regression analysis, each increase in the number of axillary nodes is

associated with a 2.7-fold increase in the odds of the participant being HIV-positive ($P = .001$), with HIV-positive participants having a maximum of 3 axillary nodes and a mean of 0.37 nodes, and HIV-negative participants having a maximum of 2 and a mean of 0.08 nodes ($P = .001$). Symmetry was not associated with HIV status (symmetry of axillary nodes in HIV-positive participants, 17 out of 29, 59%; symmetry of axillary nodes in HIV-negative participants, 3 out of 7, 43%; $P = .451$).

Inguinal Nodes (Known to Be Positive in Chronic HIV Infection). The SUVmax and size were not predictors of HIV status in the inguinal lymph nodes. However the number of inguinal lymph nodes and the symmetry was significantly associated with HIV infection (symmetry of inguinal nodes seen in HIV-positive participants, 11 out of 21, 52%; symmetry of inguinal nodes seen in HIV-negative participants, 2 out of 14, 14%; $P = .022$). The number of nodes was a significant predictor of HIV status ($P = .047$; 95%CI, 1.01–2.83; OR, 1.69) in a logistic regression and there was a significant difference in the mean number of nodes between the 2 groups with a mean of 0.6 nodes in the HIV-positive participants and a mean of 0.3 nodes in the HIV-negative participants (*t*-test: $P = .0417$).

Colic or Mesenteric Nodes (Known to Be Positive in Late-Stage HIV Infection). There were no significant associations between HIV status and the number, symmetry, SUVmax, or size of the colic, paracolic, or mesenteric lymph nodes.

Nodes Involved in Draining the Cervix. Nodes included in this analysis are paracervical, parametrial, presacral, sacral, external and internal iliac, common iliac, hypogastric, and para-aortic nodes. There were no significant relationships between HIV status and SUVmax, size, number, or symmetry in these nodes. Online supplemental Images 6a and 6b are of the HIV-positive (6a) and HIV-negative (6b) participants with the highest number of lymph nodes visualized in the pelvic region.

Additional Findings. In our sample, aortopulmonary nodes were significantly ($P = .0096$) more frequent in HIV-negative participants (mean, 0.15; SD, 0.454; 95%CI, 0.01–0.08) than in HIV-positive participants (mean, 0.05; SD, 0.217; 95%CI, 0.08–0.22), and abdominal caval nodes had higher SUVmax in HIV-negative participants (mean, 7.941) than in HIV-positive participants (mean, 5.685; $P = .0430$). Online supplemental Image 7 is of the HIV-positive participant with the largest node (3.1 cm) and the node with the highest SUV (24.38) in the head and neck region and in the thorax (SUV: 21.77; size: chain of >14 cm).

DISCUSSION

The uniformity in presentation of nodes draining the cervix in HIV-positive and HIV-negative LACC participants confirms that visualization of these nodes on ^{18}F-FDG PET/CT scans may be attributed to malignancy rather than HIV status of the participants in our sample. Overall there are some novel differences between the visualization of lymph nodes in HIV-positive and HIV-negative participants in our study, which may be of use in deciding the likely cause of the increased FDG uptake in some patients; however, the overall pattern of presentation and the nodal characteristics are similar between the two groups.

There is a significant association between higher SUVmax and larger lymph node diameter visualized in ^{18}F-FDG PET/CT. SUVmax and node size were consistently higher in the pelvis and abdomen than in the thorax and head and neck regions regardless of the HIV status. The number of nodes visualized in the pelvis was higher that than in any other region. These findings are all in line with the literature and the expected route of metastatic spread of cervical cancer (11-13). In a report by Iyengar et al. (22) on the FDG uptake in 12 patients with acute HIV infection and 11 patients with mid/chronic HIV infection, all patients presented with an FDG uptake that was greater in the cervical and axillary lymph nodes than in the inguinal and iliac chains. The patients in their study were however not all on ART, and there was a significant correlation between FDG PET signal and viral load (22). In our sample of HIV-positive cervical cancer participants, most of whom were on ART, the highest SUVmax was still seen in the pelvis and abdomen.

There is a risk of underestimating the extent of lymph node involvement in HIV-positive participants if the increased FDG uptake of a node is incorrectly attributed to HIV infection. We were therefore specifically interested in the differences in lymph node presentation between HIV-positive and HIV-negative participants in our sample.

The visualization of head and neck nodes is frequently cited in the literature as being associated with acute HIV infection (18-20, 22). The majority of participants in our study (82%) were on ART for >6 months, and the majority of these not on ART were aware of their HIV-status and were not likely to be in acute stages of HIV infection. The majority of our participants also had a CD4 count >200 cells/μL. Although more head and neck lymph nodes were visualized in the HIV-positive participants in our sample, differences in the number of head and neck nodes visualized between HIV-positive and HIV-negative participants were not significant. However, >4 nodes in the head and neck region were more likely to be seen in HIV-positive patients. Further histological evaluation of nodes in this region for malignancy in HIV-positive patients may therefore still be warranted.

Kidd et al. (6), reported that 53% of 234 patients with LACC presented with FDG-avid lymph nodes on ^{18}F-FDG PET/CT scans, and in that sample, the nodes were visualized as high as the supraclavicular region. Our sample only included participants in FIGO stages IIB to IIIB (staged clinically), and the number of participants with FDG-avid nodes in our study was considerably higher (90%), likely because of the higher proportion of our participants with more advanced stages of disease. We also saw increased FDG uptake in the supraclavicular nodes that are known to be potential sites of metastatic spread in patients with cervical cancer. In our sample however, the number of supraclavicular nodes visualized was significantly higher in the HIV-positive participants despite the management of the HIV infection with ART. Based on these findings, further assessment of supraclavicular nodes visualized in HIV-positive cervical cancer patients to rule out HIV infection as a cause of the increased FDG-uptake may be warranted.

Although axillary nodes were significantly associated with HIV infection in our sample, the relationship was not exclusive, with 6% of HIV-negative participants presenting with FDG-avid axillary nodes. The spread to axillary nodes can therefore not be conclusively excluded in HIV-positive immunocompetent patients with chronic HIV-infection who are on ART and have a CD4 count>200 cells/μL.

Symmetrical inguinal lymph nodes are more likely to be visualized in HIV-positive participants, even if their HIV infection is managed. This is in line with the literature that has found inguinal nodes to be FDG-avid during chronic HIV infection.

In HIV-positive participants, larger nodes were associated with lower CD4 counts and the only difference in size between HIV-positive and -negative participants was seen in the abdomen, where larger nodes were more common in HIV-positive participants. The literature shows a significant association between CD4 count and SUVmax (16, 17); however, we did not see the same significant association. The majority of our participants had a CD4 count >200 cells/μL and the association may therefore be more relevant to patients with a CD4 count<200 cells/μL. Based on our results it appears that the SUVmax in immunocompetent patients is a reliable measurement of metabolic activity in potentially metastatic nodes.

Fewer participants in this study were in the late stage of HIV infection, with only 7.8% of HIV-positive participants presenting with a CD4 count <200 cells/μL. The lack of colic or mesenteric nodes visualized in our sample is therefore in line with the literature (19).

Limitations

Although histology remains the gold standard for a definitive diagnosis of the nature of lymph node pathology, histological sampling of all PET-positive lymph nodes is not always ethically feasible.

CONCLUSION

Our results indicated that ^{18}F-FDG PET/CT is a reliable staging method for LACC regardless of the HIV status, provided the patients are not in acute stages of HIV infection, have a CD4 count >200 cells/μL, and/or are on ART. The results of this study are clinically relevant, as this may be of assistance in determining which lymph nodes visualized on ^{18}F-FDG PET/CT are likely to be due to metastatic spread in HIV-positive patients with LACC, and in preventing understaging of HIV-positive LACC patients.

Supplemental Materials

Supplemental Image 1: https://doi.org/10.18383/j.tom.2019.00017.sup.01

Supplemental Image 2: https://doi.org/10.18383/j.tom.2019.00017.sup.02

Supplemental Image 3: https://doi.org/10.18383/j.tom.2019.00017.sup.03

Supplemental Image 4: https://doi.org/10.18383/j.tom.2019.00017.sup.04

Supplemental Image 5: https://doi.org/10.18383/j.tom.2019.00017.sup.05

Supplemental Image 6: https://doi.org/10.18383/j.tom.2019.00017.sup.06

Supplemental Image 7: https://doi.org/10.18383/j.tom.2019.00017.sup.07

ACKNOWLEDGMENTS

Funding was obtained from the National Research Foundation of South Africa (TP12082710852). ^{18}F-FDG was supplied at a discounted rate by Radioisotopes SOC Ltd. We would like to thank all of the participants who participated in the study.

Disclosure: No disclosures to report.

Conflict of Interest: The authors have no conflict of interest to declare.

REFERENCES

1. Boellaard R, Delgado-Bolton R, Oyen WJG, Giammarile F, Tatsch K, Eschner W, Verzijlbergen FJ, Barrington SF, Pike LC, Weber WA, Stroobants S, Delbeke D, Donohoe KJ, Holbrook S, Graham MM, Testanera G, Hoekstra OS, Zijlstra J, Visser E, Hoekstra CJ, Pruim J, Willemsen A, Arends B, Kotzerke J, Bockisch A, Beyer T, Chiti A, Krause BJ. FDG PET/CT: eANM procedure guidelines for tumour imaging: version 2.0. Eur J Nucl Med Mol Imaging. 2015;42:328–354.
2. Hansen HV, Loft A, Berthelsen AK, Christensen IJ, Høgdall C, Engelholm SA. Survival outcomes in patients with cervical cancer after inclusion of PET/CT in staging procedures. Eur J Nucl Med Mol Imaging. 2015;42:1833–1839.
3. Magné N, Chargari C, Vicenzi L, Gillion N, Messai T, Magné J, Bonardel G, Haie-Meder C. New trends in the evaluation and treatment of cervix cancer: the role of FDG PET. Cancer Treatment Reviews. 2008;34:671–681.
4. Sun Y, Lu P, Yu L. The volume-metabolic combined parameters from 18 F-FDG PET/CT may help predict the outcomes of cervical carcinoma. Acad Radiol. 2016;23:605–610.
5. Morkel M, Ellmann A, Warwick J, Simonds H. Evaluating the role of f-18 fluorodeoxyglucose positron emission tomography/computed tomography scanning in the staging of patients with stage IIIB cervical carcinoma and the impact on treatment decisions. Int J Gynecol Cancer. 2018;28:379–384.
6. Kidd EA, El Naqa I, Siegel BA, Dehdashti F, Grigsby PW. FDG-PET-based prognostic nomograms for locally advanced cervical cancer. Gynecol Oncol. 2012;127:136–140.
7. Joo JH, Kim YS, Nam J. Prognostic significance of lymph node ratio in node-positive cervical cancer patients. Medicine (Baltimore). 2018;97:e11711.
8. Kidd EA, Siegel BA, Dehdashti F, Rader JS, Mutch DG, Powell MA, Grigsby PW. Lymph node staging by positron emission tomography in cervical cancer: relationship to prognosis. J Clin Oncol. 2010;28:2108–2113.
9. Crivellaro C, Signorelli M, Guerra L, De Ponti E, Buda A, Dolci C, Pirovano C, Todde S, Fruscio R, Messa C. 18F-FDG PET/CT can predict nodal metastases but not recurrence in early stage uterine cervical cancer. Gynecol Oncol. 2012;127:131–135.
10. Driscoll DO, Halpenny D, Johnston C, Sheehy N, Keogan M. 18F-FDG-PET/CT is of limited value in primary staging of early stage cervical cancer. Abdom Imaging. 2015;40:127–133.
11. da Silva LP, Moreira CMM, Amorim MHC, et al. Contextual quality of life of HIV-positive patients with cervical carcinoma at Tygerberg Hospital. AIDS Care. 2014;28:1–8.
12. Benedetti-Panici P, Maneschi F, Scambia G, Greggi S, Cutillo G, D'Andrea G, Rabitti C, Coronetta F, Capelli A, Mancuso S. Lymphatic Spread of Cervical Cancer: An anatomical and pathological study based on 225 radical hysterectomies with systematic pelvic and aortic lymphadenectomy. Gynecologic Oncology . 1996;62(1):19–24.
13. Höckel M, Horn L, Tetsch E, Einenkel J. Pattern analysis of regional spread and therapeutic lymph node dissection in cervical cancer based on ontogenetic anatomy. Gynecol Oncol. 2012;125:168–174.
14. Stadalnik RC, Bakheet SM, Powe J. Benign causes of 18-FDG uptake on whole body imaging. Semi Nucl Med. 1998;28:352–358.
15. Bental M, Deutsch C. Metabolic changes in activated T cells: an NMR study of human peripheral blood lymphocytes. Magn Reson Med. 1993;29:317–326.
16. Cloyd MW, Chen JJ, Wang I. How does HIV cause AIDS? The homing theory. Mol Med Today. 2000;6:108–113.
17. Dimopoulos Y, Moysi E, Petrovas C. The lymph node in HIV pathogenesis. Curr HIV/AIDS Rep. 2017;14:133–140.
18. Davison JM, Subhramaniam RM, Surasi DS, Cooley T, Mercier G, Peller PJ. FDG PET/CT in patients with HIV. AJR Am J Roentgenol. 2011;197:284–294.
19. Scharko AM, Perlman SB, Pyzalski RW, Graziano FM, Sosman J, Pauza CD. Whole-body positron emission tomography in patients with HIV-1 infection. Lancet. 2003;362:959–961.
20. Sathekge M, Maes A, Kgomo M, Van De Wiele C. Fluorodeoxyglucose uptake by lymph nodes of HIV patients is inversely related to CD4 cell count. Nucl Med Commun. 2010;31:137–140.
21. Brust D, Polis M, Davey R, Hahn B, Bacharach S, Whatley M, Fauci AS, Carrasquillo JA. Fluorodeoxyglucose imaging in healthy subjects with HIV infection : impact of disease stage and therapy on pattern of nodal activation. AIDS. 2006;20:985–993.
22. Iyengar S, Chin B, Margolick JB, Sabundayo BP, Schwartz DH. Anatomical loci of HIV-associated immune activation and association with viraemia. Lancet. 2003;362:945–950.